

Synthesis and use of alumina nanoparticles as an adsorbent for the removal of Zn(II) and CBG dye from wastewater

Rompicherla J. Bhargavi · Utkarsh Maheshwari · Suresh Gupta

Received: 24 September 2014 / Accepted: 9 December 2014 / Published online: 18 December 2014
© The Author(s) 2014. This article is published with open access at Springerlink.com

Abstract In the present study, an alumina nanoparticle adsorbent is developed using solution combustion synthesis method and is further utilized for the removal of zinc (Zn(II)) and color black G (CBG) from wastewater. The developed adsorbent is characterized using SEM–EDS technique. The effect of various parameters such as the initial concentration, the contact time, the mass of adsorbent and the solution pH are studied for the removal of Zn(II) and CBG. The equilibrium time for both, Zn(II) and CBG is obtained to be approximately 4.5 h. The maximum adsorption of Zn(II) is found at pH value of 7 while the maximum removal of CBG is obtained at pH value of 2. The Langmuir isotherm model is found suitable for explaining the adsorption behavior of Zn(II) ($R^2 = 0.976$) and CBG ($R^2 = 0.974$) onto alumina nanoparticles, which supports the monolayer formation of Zn(II) and CBG during the adsorption process. The maximum adsorbent capacity of alumina nanoparticles for the removal of Zn(II) and CBG are obtained as 1,047.83 and 263.16 mg g⁻¹, respectively. The kinetic data obtained during the experiments are better fitted with the pseudo-first-order model for both, Zn(II) ($R^2 = 0.989$) and CBG ($R^2 = 0.971$). A statistical analysis is also carried out to develop the mathematical equation which relates the different independent parameters (initial metal concentration, pH, time and mass of adsorbent) with the dependent parameter (adsorption

capacity). The optimum values of independent parameters are estimated using Microsoft Solver.

Keywords Adsorption · Dye · Zinc · Textile

Introduction

In the last few decades, with an increase in the urbanization and industrialization, there is an increase in the use of heavy metals and dyes in the industries. Industries such as electroplating, galvanizing, pigments, mine drainage, etc. are using metals in their processing. Other industries such as textile, ink, paper and pulp, leather, etc. are using significant amount of dyes in their processing. These industries are releasing a huge quantity of effluent which is contaminated with different types of metals and dyes and is responsible for polluting our water bodies [1, 2].

Textile industries are the key industries which are discharging both, metals and dyes to the environment through their effluent. The metals such as Zn(II), Cr(VI), Cu(II), etc. and dyes such as Color Black G, Congo Red, Malachite Green, etc. are the ones which are very much toxic and are primarily present in the effluents of the textile effluents [1, 3–9]. Hence, an emphasis is required for handling the effluents from textile industries.

The textile industry effluent, contaminated with metals and dyes, is required to be treated before it is released into the water bodies. There are various methods available for the removal of metals and dyes, such as adsorption [10, 11], photo-degradation [12–14], ion exchange [15], oxidation [16], etc. Among these available methods, adsorption is proven to be an economical and efficient method which may be feasible for industrial scale operation [17]. The adsorbents required to adsorb metal and dyes from

R. J. Bhargavi · U. Maheshwari · S. Gupta (✉)
Department of Chemical Engineering, Birla Institute
of Technology and Science (BITS), Pilani 333031,
Rajasthan, India
e-mail: sureshg@pilani.bits-pilani.ac.in

U. Maheshwari
e-mail: utkarsh@pilani.bits-pilani.ac.in

these industry effluents are required to have properties such as higher surface area, high thermal stability and small pore diameters.

There is a considerable change observed in the chemical, physical, mechanical and optical properties of the adsorbents when the particle size is scaled down to a nano level. The principal change is observed on the surface area of the nanomaterial which increases tremendously and leads to the higher adsorption capacity for the heavy metals and dyes removal [10]. The change in the structure of the pore is also an important attribute. This will correspond to the faster transportation of the metal ions or dyes to the internal active sites of adsorbents. These changes in the properties of nanoadsorbent make them suitable and efficient for the treatment of textile industry effluents. Hence, there is a dire need to develop the nanoadsorbent for the removal of multiple pollutants from the effluent streams of textile industries. Recently, various nanomaterials such as Single-Walled Carbon Nanotubes (SWCNTs), Multi-Walled Carbon Nanotubes (MWCNT), Polymer Nanocomposites, Nano-sized γ -Fe₂O₃, Gold nanoparticles, Iron & Titanium nanoparticles, Titanium nanoparticles, Silver nanoparticles and alumina-based nanoparticles, etc. have been developed and used as adsorbents [10, 18].

There are a number of adsorbents reported in the literature which are used for the adsorption of multiple metal ions from wastewater. Some of the examples are the functionalized Carbon Nanotubes (CNTs) and activated neem bark for the adsorption of a toxic hexavalent chromium ion [7, 19], carbon nanotube along with magnesium oxide form composite for the removal of Pb(II) [20], fertilizer wastes to adsorb multiple metal ions [21], alumina-coated carbon nanotubes for the Pb(II) removal [22], nickel oxide for the removal of Zn(II), Co(II) and Cd(II) [23], orange peel for the cadmium removal [24], humic acid (HA) for Cu(II) and Zn(II) from aqueous solution [25], zinc oxide nanoparticles (ZnO) for the adsorption of Zn(II), Cd(II) and Hg(II) [26], clay minerals in surficial sediment samples for the removal of Cu(II) and Zn(II) [27].

Similarly, a number of adsorbents are reported in the literature for the removal of dyes from the effluent of industries. Azo dyes are the primary class of dyes, having a number of industrial applications. Various adsorbents are utilized for the removal of these azo dyes from the industrial effluents, e.g. functionalized multi-walled carbon nanotubes (f-MWCNTs) have been applied for the adsorption and decolorization of three different azoic dyes viz. Direct Congo Red, Reactive Green HE4BD and Golden Yellow MR dyes [28], magnetic-modified multi-walled carbon nanotubes have been employed for the removal of Crystal Violet (CV), Thionine (Th), Janus Green B (JG), and Methylene Blue (MB) dyes [29], two

bamboo-derived carbons BACX2 and BACX6 for the removal of a large reactive dye and Reactive Black 5 [28]. Previous studies have also reported the use of different waste materials for the removal of dyes [4, 30–33].

Most of the studies reported in the literature are limited to the use of developed adsorbents for the adsorption of either metals or dyes. Very few studies have been reported for the use of any adsorbent for the removal of both dyes and metals (Table 2). As the Zn(II) and CBG are the major components of the effluent released from textile industries, thus, there is a necessity to develop a suitable adsorbent for the efficient removal of Zn(II) and CBG from waste water.

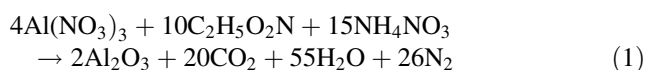
In the present work, the solution combustion synthesis method is utilized for the development of alumina nanoparticles. This developed adsorbent is used for the removal of Zn(II) and CBG from wastewater. The effect of various parameters such as the initial concentration, contact time, adsorbent dosage and pH of the solution are studied for the removal of Zn(II) and CBG. Various isotherm and kinetic models are being applied using the equilibrium and kinetic experimental data. A mathematical correlation is developed using obtained experimental results and utilized for estimating the optimum values of different parameters using Microsoft Solver.

Materials and methods

Synthesis of nanoadsorbent

There are a number of methods available for the synthesis of the nanomaterials. Combustion Synthesis (CS) or Self-propagating High-temperature Synthesis (SHS) is one of them, which is an energy saving and eco-friendly process for the production of low-cost nanoadsorbents. On the basis of the physical nature of their primary reaction medium, the process can be further divided into three methods: (1) condensed phase combustion where the reactants are in solid state, (2) solution combustion synthesis where the reaction medium is an aqueous solution and (3) gas phase combustion [34].

Alumina-based nanoparticles using alumina as a base are synthesized by the solution combustion synthesis. Glycine and ammonium nitrate with nitrate as the basic raw material are used for the process [35]. The oxidizer to fuel ratio for the nanoaluminium production is maintained at 1:1. The solution combustion reaction is carried out in a muffle furnace at temperatures <45 °C. Assuming the complete combustion during the process, the theoretical equation for the aluminium combustion synthesis can be written as Eq. 1 [35].



All the chemicals used for the synthesis and experimental studies are of the analytical grade from Merck.

Characterization of adsorbent

The developed alumina nanoparticles adsorbent is characterized using Scanning Electron Microscopy (SEM) and Energy Dispersive X-ray Spectroscopy (EDS) (INCA). The SEM image helps in analyzing the morphology and size of the particles of the developed adsorbent. The EDS analysis helps in identifying the elements present on the surface of the nanoparticles.

Batch experiments

The stock solutions of 1,000 mg L⁻¹ of Zn(II) and CBG are prepared by dissolving stoichiometric amount of ZnSO₄·7H₂O and CBG dye in distilled water. The solutions are further diluted using distilled water to obtain the required standard solutions from a range of 50–1,000 mg L⁻¹.

Batch experiments are performed by agitating the prepared solution flasks for a predetermined period at room temperature (35 ± 2 °C) on a rotary shaker. The effect of contact time is studied at room temperature (35 ± 2 °C) with an adsorbent dosage of 0.4 g L⁻¹ for the initial concentration of Zn(II) and CBG as 500 and 100 mg L⁻¹, respectively. The equilibrium study is performed by varying initial concentrations from 100 to 900 and 50–500 mg L⁻¹ of Zn(II) and CBG, respectively, while maintaining the constant adsorbent dosage and contact time at 0.4 g L⁻¹ and 4.5 h, respectively, for each sample. The effect of adsorbent dosage is studied by performing experiments at room temperature by varying the mass of adsorbent from 0.4 to 2.0 g L⁻¹ in a sample of 1,000 and 200 mg L⁻¹ of Zn(II) and CBG solutions, respectively. The effect of pH is also studied by conducting experiments for a variation of pH from 2 to 7 by keeping the initial concentration of the solution at 400 and 100 mg L⁻¹ of Zn(II) and CBG solution, respectively, and maintaining the adsorbent dosage of 0.4 g L⁻¹. All the experiments are done twice to check the repeatability of the process and the average values are used for evaluating various parameters.

Analysis of Zn(II) and CBG

The concentration of dye left in the liquid solution is determined using a UV–Visible spectrophotometer (Evolution 201, Thermo Scientific) while the amount of the Zn(II) is determined using the EDTA titration method [36].

The amount of Zn (II) or CBG adsorbed by the developed alumina nanoparticles are calculated using the following Eq. 2.

$$q_e = \frac{(C_0 - C_e)V}{W} \quad (2)$$

where q_e is the amount of Zn(II) or CBG adsorbed by the adsorbent (mg g⁻¹), C_0 is the initial liquid phase concentration of Zn(II) or CBG (mg L⁻¹), C_e is the liquid phase concentration of Zn(II) or CBG at equilibrium (mg L⁻¹), V is the initial volume of Zn(II) or CBG solution (ml) and W is the weight of the adsorbent (g) [7].

Results and discussion

Characterization

The developed adsorbent is characterized using SEM and EDS analysis. The SEM image for the developed adsorbent is shown in Fig. 1a. The SEM image shows a clear surface available for the adsorption. This image also indicates the availability of nano-size pores and cracks on the surface of adsorbent which may be one of the reasons for the significant increase in the adsorption capacity of the developed adsorbent. The EDS analysis for the developed adsorbent is shown in Fig. 1b. This analysis shows the peaks of C, Al and O atoms and confirms the presence of Al₂O₃ nanoparticles. The presence of C, Al and O are in accordance with the Eq. 1 of the synthesis.

Effect of contact time

The effect of contact time on the removal of Zn(II) and CBG are studied and presented in Fig. 2. Figure 2a and b indicates that the percentage removal for Zn (II) and CBG increases with an increase in contact time. It can also be inferred that the rate of adsorption of Zn(II) and CBG is decreasing with increase in the contact time. The change in the percentage removal is only 1 and 0.9 % for Zn(II) and CBG, respectively, beyond the 4 h of contact time which is not significant. Therefore, the equilibrium time is considered to be approximately 4.5 h for Zn(II) and CBG and is selected for the remaining batch experiments.

A similar trend of increase in the adsorption capacity is also observed with an increase in contact time. With an increase in the contact time, the time required for diffusion of Zn(II) and CBG molecules to the internal adsorption sites is sufficient. This leads to the utilization of more and more adsorption sites with increase in time and results in increase in the adsorption capacity and percentage removal with time. The maximum percentage removal for Zn(II) and CBG is obtained as 33.5 and 25.6 %, respectively.



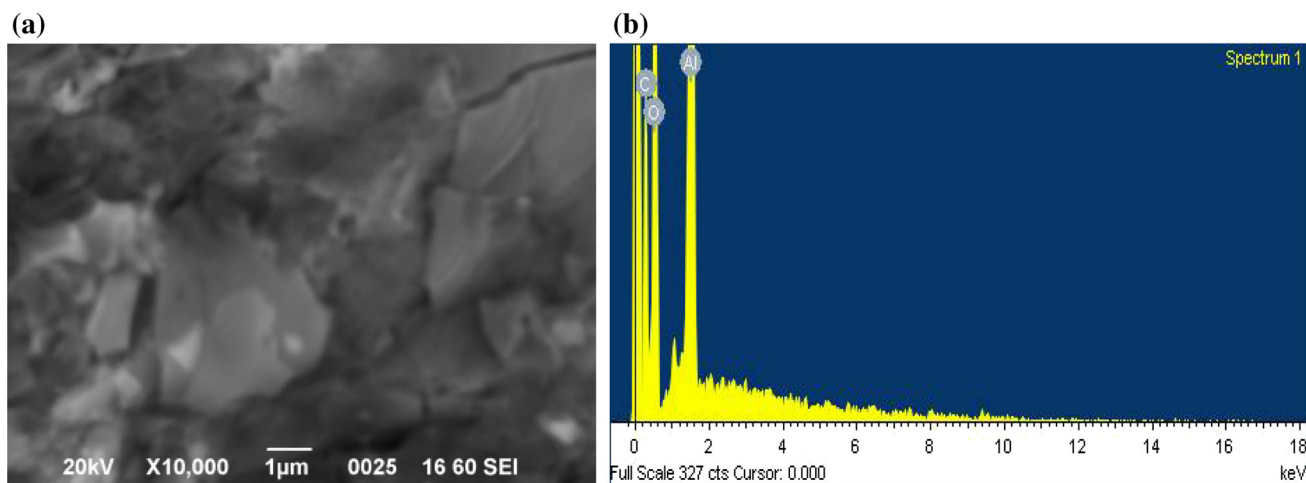


Fig. 1 a SEM b EDS analysis of developed alumina nanoparticles adsorbent

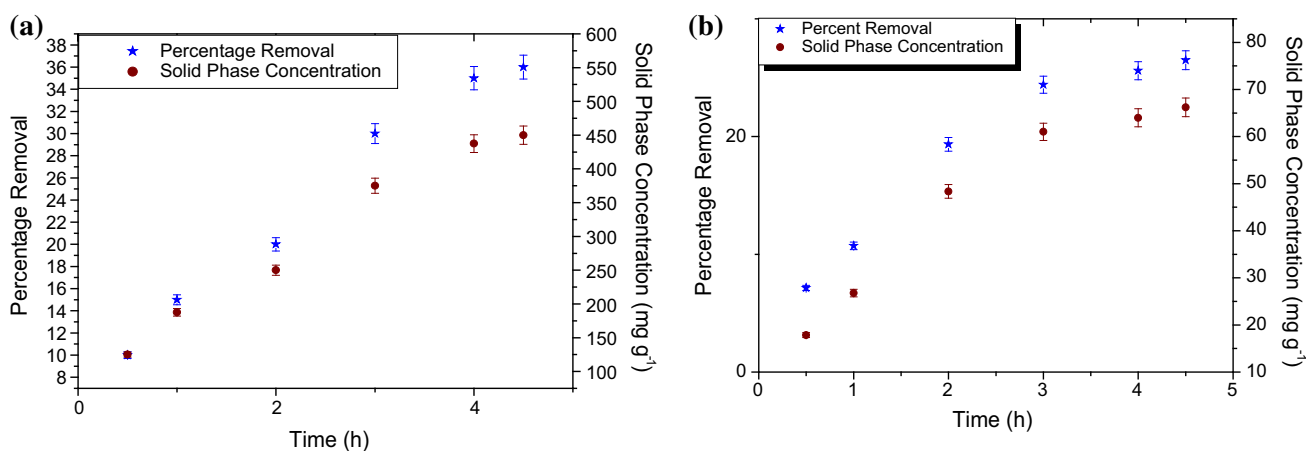


Fig. 2 Percent removal Vs time (hrs) for 0.4 g L⁻¹ adsorbent for a 500 mg L⁻¹ Zn(II) and b 100 mg L⁻¹ CBG

Effect of initial concentration

The effect of initial concentration on the removal of Zn(II) and CBG is shown in Fig. 3. The initial concentrations vary from 100 to 900 and 50–500 mg L⁻¹ for Zn(II) and CBG, respectively. It can be inferred from the Fig. 3a and b that the percent removal is decreasing from 50 to 28.89 and 66.67–19.34 % with an increase in the initial concentration from 100 to 900 and 50–500 mg L⁻¹ for Zn(II) and CBG, respectively. Also, it is found that the solid phase concentration of the adsorbent is increased from 125 to 650 and 83.33–241.82 for Zn(II) and CBG, respectively, with increase in initial concentration.

The decrease in the percentage removal with an increase in inlet concentration is due to the unavailability of sufficient number of active sites required for the adsorption process. As the inlet concentration is increasing, more amount of solute is available for adsorption in the fixed

number of active sites which results in the increase of the adsorption capacity of the adsorbent.

Effect of adsorbent dosage

Figure 4 shows the effect of adsorbent dosage on the removal of Zn(II) and CBG. The mass of the adsorbent is varied from 0.4 to 2.2 mg L⁻¹ keeping other parameters such as contact time (4.5 h) and initial concentration (1,000 and 200 mg L⁻¹ for Zn(II) and CBG, respectively) constant. With an increase in the adsorbent dosage from 0.4 to 2.2 gm L⁻¹, the percent removal of Zn(II) and CBG increased from 53.33 to 71 and 42.86 to 64.88 %, respectively. With an increase in the adsorbent dosage, there is a decrease in the solid phase concentration of the adsorbent from 1,333.33 to 322.73 and 107.14 to 29.49 mg g⁻¹ for the removal of Zn(II) and CBG, respectively.

The increase in the percentage removal is due to the availability of more number of active sites for the removal of Zn(II) and CBG. As the amount of adsorbent is increased while keeping the same amount of solute in solution, adsorption capacity decreases due to the unutilized adsorption sites.

Effect of pH

The effect of pH on the removal of Zn(II) and CBG is studied and presented in Fig. 5. The pH of the solution is varied from 2 to 7 while keeping inlet concentration, contact time and adsorbent dosage as 1,000 for Zn(II) & 500 mg L⁻¹ for CBG, 4.5 h and 0.4 g L⁻¹, respectively, during the experiment. It is found that the percent removal of Zn(II) increases from 12 to 44.4 %, while the removal of CBG decreases from 34.04 to 5.12 % with an increase in the pH of the solution from 2 to 7.

With an increase in pH value of the solution, there is no significant difference noted in the removal of CBG. This suggests that the pH is not a regulating factor in the removal of CBG. However, a considerable increase in the percentage removal of Zn(II) has been noted with an increase in pH from 2 to 7. This indicates that the adsorption removal of Zn(II) is more favorable at higher pH.

Theoretical studies

Isotherm study

In the present study, Langmuir and Freundlich isotherm models are employed to explain the adsorption phenomenon for the removal of Zn (II) and CBG using alumina nanomolecules.

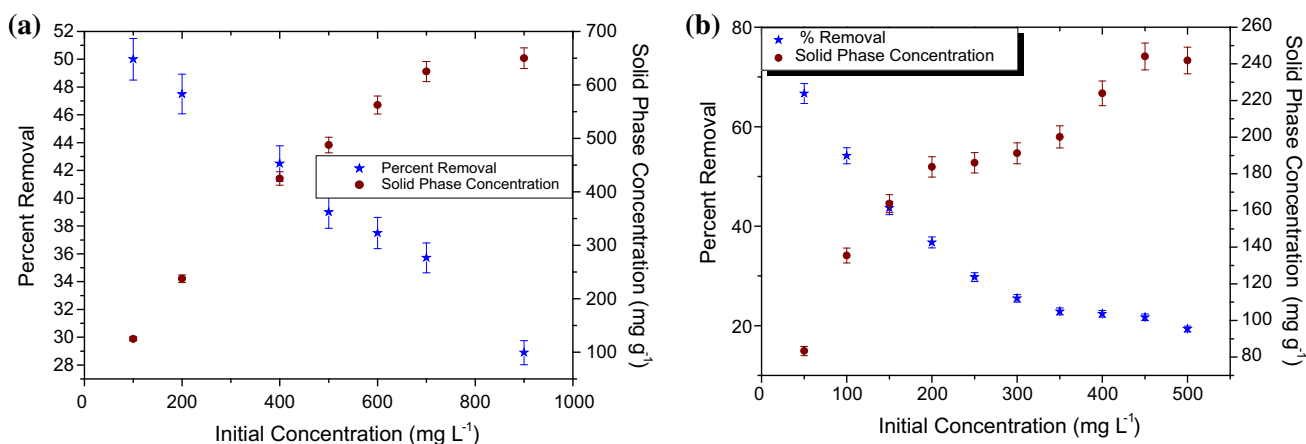


Fig. 3 Effect of initial concentration on the removal of **a** Zn(II) and **b** CBG

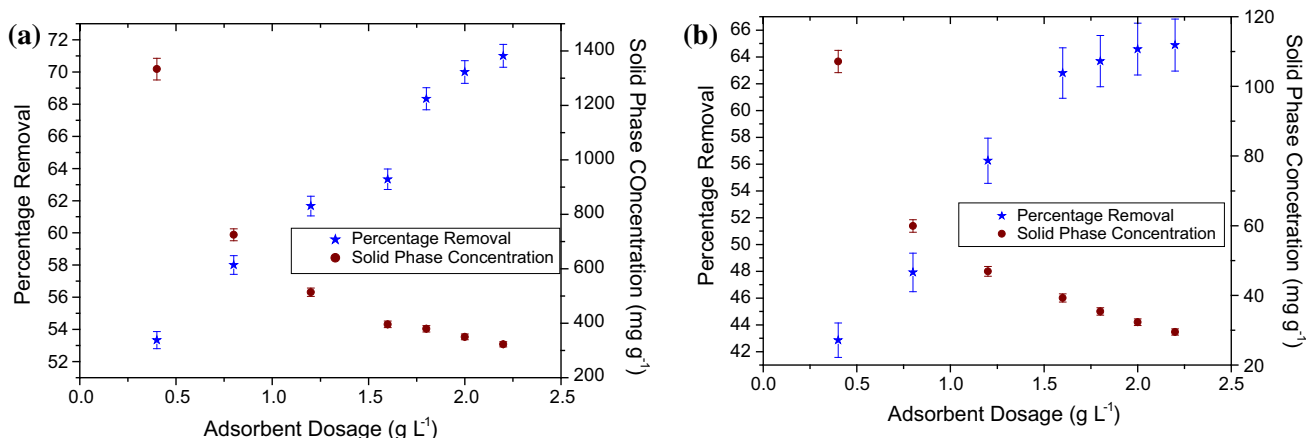


Fig. 4 Effect of adsorbent dosage for the removal of **a** 1,000 mg L⁻¹ Zn(II) and **b** 200 mg L⁻¹ CBG

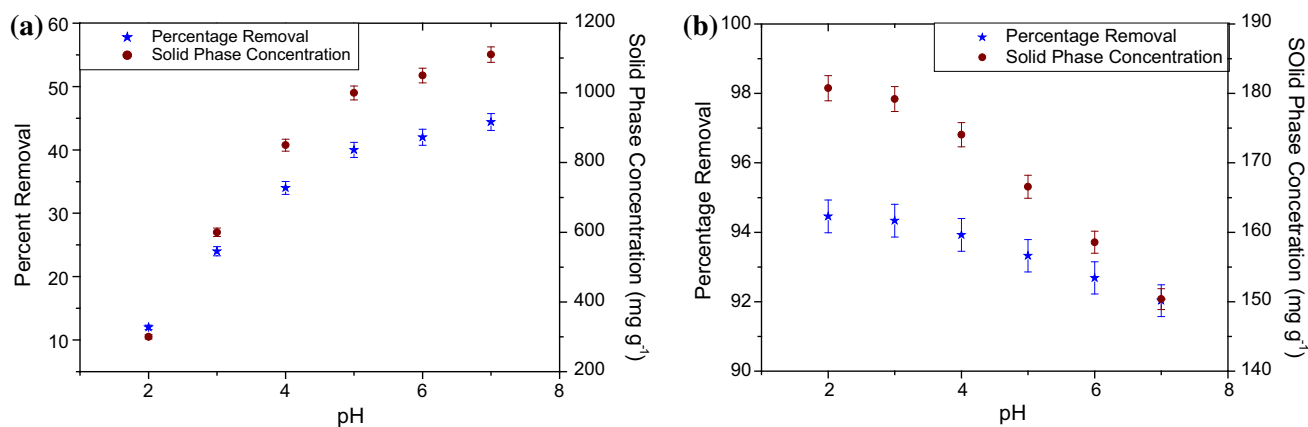


Fig. 5 Effect of pH on the removal of **a** 1,000 mg L⁻¹ Zn(II) and **b** 500 mg L⁻¹ CBG

Langmuir isotherm model

The Langmuir isotherm model is a widely used isotherm model in the literature. The model assumes the formation of monolayer during the removal of metal/dye from aqueous solution using developed nanoaluminium adsorbent. The Langmuir isotherm study also provides the maximum adsorption capacity of the adsorbent for the removal of metal/dye [11, 37]. The linearized Langmuir isotherm model is expressed as given in Eq. 3.

$$\frac{C_e}{q_e} = \frac{1}{q_m b} + \frac{C_e}{q_m} \quad (3)$$

where b is adsorption equilibrium constant (L mg⁻¹) related to the apparent energy of adsorption and q_m is the maximum quantity of adsorbate required to form a single monolayer on unit mass of adsorbent (mg g⁻¹).

The equilibrium experimental data are plotted between C_e/q_e and C_e as shown in Fig. 6 for the removal of Zn(II) and CBG. The correlation coefficients and the model parameters are evaluated and tabulated in Table 1.

Freundlich isotherm model

The Freundlich model suggests a heterogeneous adsorption of the solute on the adsorbent surface [38]. The model is expressed by the following Eq. 4.

$$q_e = K_F C_e^{\frac{1}{n}} \quad (4)$$

where K_F is representing the Freundlich constant, which is indicating the relative adsorption capacity of the adsorbent related to the bonding energy and n is the heterogeneity factor representing the deviation from linearity of adsorption and is also known as Freundlich coefficient.

The Eq. 4 can be linearized and expressed as Eq. 5.

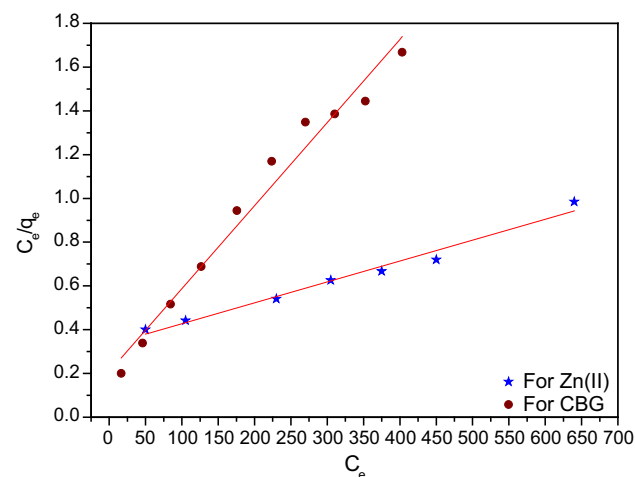


Fig. 6 Langmuir isotherm plot for the removal of Zn(II) and CBG

Table 1 Isotherm parameters for the removal of Zn(II) and CBG

	Langmuir isotherm parameters			Freundlich isotherm parameters		
	b	q_m (mg g ⁻¹)	R^2	K_F	n	R^2
Zn(II)	0.002875	1,047.83	0.976	9.86711	1.4836	0.971
CBG	0.01832	263.16	0.974	38.4902	3.245	0.953

$$\log q_e = \log K_F + \frac{1}{n} \log C_e \quad (5)$$

The experimental data are plotted between $\log q_e$ and $\log C_e$ and shown in Fig. 7 for the removal of Zn(II) and CBG. The coefficients for Freundlich isotherm are evaluated and tabulated in Table 1.

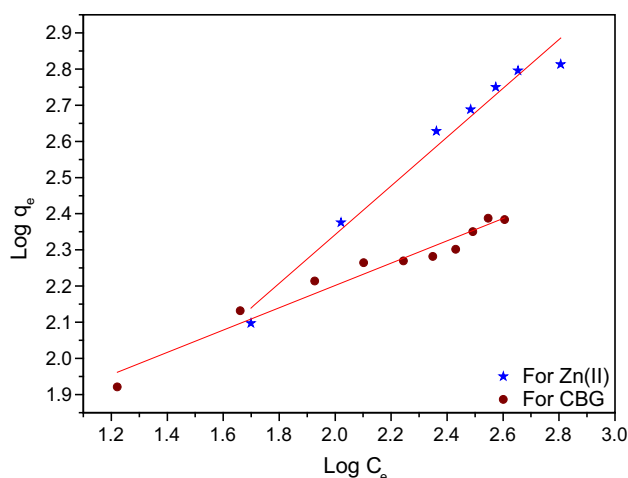


Fig. 7 Freundlich isotherm for the removal of Zn(II) and CBG

Final remarks on isotherm study

On studying and validating the experimental data with the Langmuir and Freundlich isotherm models, it is found that the removal of Zn (II) and CBG are well explained by the Langmuir isotherm model. This suggests that the adsorption is primarily governed by the formation of the monolayer on the adsorption sites. The maximum adsorption capacity (i.e. 1,047.83 and 263.16 mg g⁻¹ for Zn(II) and CBG removal, respectively) found by the Langmuir model is much higher as compared for other adsorbents used for the removal of heavy metals and dyes. The adsorption capacity obtained for the removal of Zn(II) and CBG is

compared with other nanoadsorbents utilized for the removal of metal or dyes and are tabulated in Table 2.

The evaluation of the equilibrium study is an essential factor for the designing of the fixed-bed adsorption column. This study helps in understanding the interaction of the concentration of the solute on the solid and liquid phase, which works as the driving force during the continuous adsorption process. The equilibrium study also helps in characterizing the shape of the breakthrough curve which is a very important factor in the designing of the fixed-bed adsorption column. Maximum fraction of bed length is possibly utilized during the continuous operation as the unused bed length is less for a favorable isotherm.

Kinetic study

In the present work, pseudo-first-order and second-order kinetic models are employed to explain the kinetic behavior of the operation.

Pseudo-first-order kinetic model

The pseudo-first-order kinetic model is represented by the non-linear equation shown in Eq. 6 [43–45].

$$\frac{dq_t}{dt} = k_{ad} (q_e - q_t) \quad (6)$$

where q_e and q_t are the Zn(II) and CBG concentration in solid phase at equilibrium and at time t , respectively. k_{ad} is the rate constant for the pseudo-first-order adsorption

Table 2 Comparison of adsorption capacities for the removal of different metals and dyes

Adsorbents	Metal	Capacity (mg g ⁻¹)	Dye	Capacity (mg g ⁻¹)	References
Alumina nanoparticles	Zn(II)	1,047.83	CBG	263.16	Present study
Multi-walled CNT	–	–	Direct congo red	148	[28]
			Reactive green HE4BD	152	
			Golden yellow MR	141	
Succinyl-grafted chitosan	Zn(II)	290	Cationic Dye	431	[39]
Malachite NPs.	–	–	Fluorescein (Flu)	32.46	[40]
			Rhodamine B (RB)	23.47	
			Rhodamine 6G (R6G)	8.40	
Iron oxide nanoparticles	Pb(II)	167.36	–	–	[17]
Pectin–iron oxide magnetic nanocomposite	Cu(II)	48.99	–	–	[41]
Magnetic-modified multi-walled carbon nanotubes	–	–	Crystal violet (CV)	227.7	[29]
			Janus green B (JG)	250.0	
			Thionine (Th)	36.4	
			Methylene blue (MB)	48.1	
Brazilian pine-fruit shells (<i>Araucaria angustifolia</i>)	–	–	Remazol black B (RB)	74.6	[42]
Magnetic nano adsorbent	Cd(II)	35.71	–	–	[24]
Orange peel powder		50			

process. The integrated rate law after application of the initial condition of $q_t = 0$ at $t = 0$, is given by Eq. 7.

$$\log(q_e - q_t) = \log q_e - \frac{k_{ad} t}{2.303} \quad (7)$$

A linear plot is drawn between $\log(q_e - q_t)$ and t for Zn(II) and CBG experimental data and are shown in Fig. 8. A linear fit to the plot is used to evaluate the value of the rate constant k_{ad} and is tabulated in Table 3.

Second-order kinetic model

The second-order kinetic model is also utilized to explain the kinetic behavior of the operation. The applicability of the second-order kinetics is represented by the Eq. 8 [44, 45].

$$\frac{dq_t}{dt} = k_2(q_e - q_t)^2 \quad (8)$$

where q_e and q_t are representing the Zn(II) and CBG ion concentration in the solid adsorbent at equilibrium and at time t , respectively. k_2 is representing the second-order rate constant in $\text{g mg}^{-1} \text{min}^{-1}$ for the adsorption process. The integrated rate law after application of the initial condition of $q_t = 0$ at $t = 0$, is given by Eq. 9.

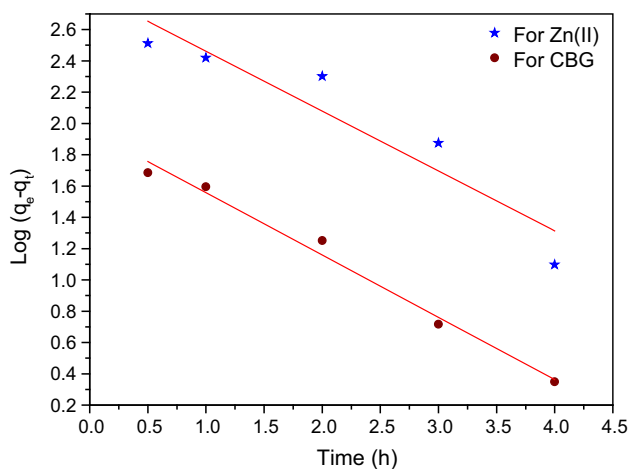


Fig. 8 Pseudo-first-order kinetic model for the removal of Zn(II) and CBG

Table 3 Kinetic parameters for the removal of Zn(II) and CBG

	First order		Second order	
	k_{ad}	R^2	k_2	R^2
Zn(II)	0.7285	0.989	0.00415	0.606
CBG	0.98789	0.97104	0.07792	0.80958

$$\frac{1}{(q_e - q_t)} = \frac{1}{q_e} + k_2 t \quad (9)$$

The experimental kinetic data for Zn(II) and CBG are plotted between $1/(q_e - q_t)$ and t and are shown in Fig. 9. The second-order rate constants are evaluated and are tabulated along with their coefficient of correlations in Table 3.

Final remarks on the kinetic study

The validation of the kinetic models using the experimental results and the obtained values of the coefficients of determination (R^2) suggests the applicability of pseudo-first-order kinetics for the adsorption of Zn(II) and CBG onto the nanoalumina adsorbent. The evaluation of the kinetic constants is important for the designing of the fixed-bed adsorption column as it will also provide the idea about the rate of adsorption. The various design parameters for the fixed-bed adsorption column such as the breakthrough time and the shape of the breakthrough curve are dependent on the rate of adsorption. If the rate of adsorption is fast, the shape of the breakthrough curve would be steep and the fraction of utilized bed would be higher.

Statistical analysis

Formulation of model

The process could be effectively utilized if the optimal conditions of the parameters would be used to perform the experiments. To find the optimum parameters, a fourth order polynomial equation is developed to correlate the dependent parameter with the independent parameters and is represented by Eq. 10.

$$q_{pre} = a_0 + \sum a_{i1} X_i + \sum a_{i2} X_i^2 + \sum a_{i3} X_i^3 + \sum a_{i4} X_i^4 \quad (10)$$

All parameters used in the Eq. 10 are normalized by considering the highest value of the parameter used in the experiment as the basis. This equation is utilized to predict the adsorption capacity (dependent parameter) using the inlet concentration (C_{in}), pH, contact time and adsorbent dosage as independent parameters.

The model is obtained by performing regression using Microsoft Excel 2007. The q_{pre} is representing the predicted value of the adsorption capacity, a_0 is the constant, a_{i1} , a_{i2} , a_{i3} and a_{i4} are the constants for the i th parameter for 1st, 2nd, 3rd and 4th order, respectively.

The regression of the experimental values for the removal of Zn(II) and CBG leads to a mathematical equations which are provided in Eqs. 11 and 12, respectively.

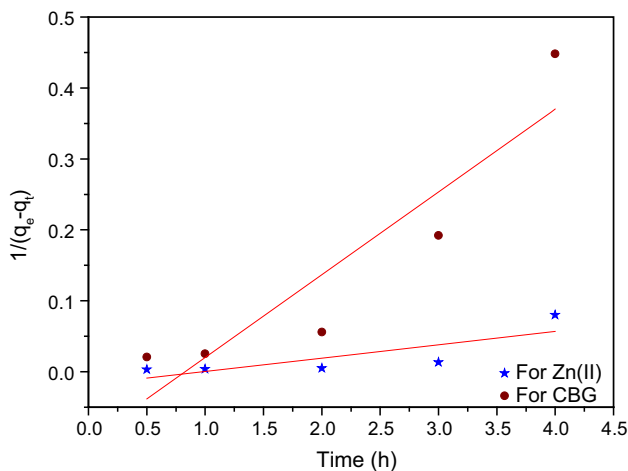


Fig. 9 Second-order-kinetic model for the removal of Zn(II) and CBG

$$\begin{aligned}
 q_{pre} = & -2.1435 - 2.0947 X_1 + 8.4548 X_2 + 4.5890 X_3 \\
 & - 1.4469 X_4 + 11.8719 X_1^2 - 18.1875 X_2^2 \\
 & - 29.1849 X_3^2 + 13.9369 X_4^2 - 19.3174 X_1^3 \\
 & + 20.0193 X_2^3 + 53.3142 X_3^3 - 31.0727 X_4^3 \\
 & + 10.1927 X_1^4 - 8.3333 X_2^4 - 32.0513 X_3^4 \\
 & + 21.6557 X_4^4 \tag{11}
 \end{aligned}$$

$$\begin{aligned}
 q_{pre} = & -2.0462 + 3.9734 X_1 + 16.5155 X_2 - 10.3049 X_3 \\
 & + 5.6137 X_4 - 10.4286 X_1^2 - 36.4521 X_2^2 \\
 & + 23.0546 X_3^2 - 21.5198 X_4^2 + 13.1761 X_1^3 \\
 & + 34.2975 X_2^3 - 22.4962 X_3^3 + 32.5672 X_4^3 \\
 & - 5.7632 X_1^4 - 11.7906 X_2^4 + 7.9803 X_3^4 \\
 & - 16.0248 X_4^4 \tag{12}
 \end{aligned}$$

The ANOVA analysis of the regression indicates that the value of *P* for all the constants is >0.0001. Hence, all the constants are equally important to evaluate the value of adsorption capacity, for the removal of Zn(II) and CBG.

Validation of model

The developed models are validated using experimental results. The graph is plotted for the actual and predicted adsorption capacity and is shown in Fig. 10.

The Fig. 10 shows that the developed models are validated very well with the experimental results and the values of *R*² is found to be 0.9696 and 0.9236 for the Zn(II) and CBG models, respectively.

Optimization

The optimization of the developed model can be very much helpful in estimating the optimum parameters which are

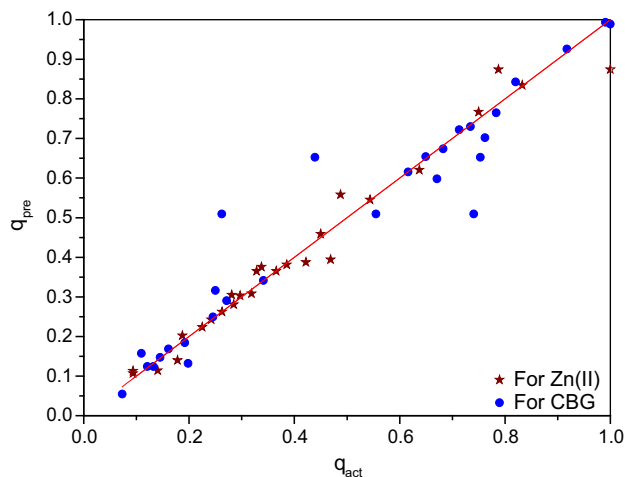


Fig. 10 Comparability of the values of adsorption capacity for the actual versus the model predicted values

Table 4 Boundary conditions for the optimization of the model

	Zn(II)		CBG	
	Minimum	Maximum	Minimum	Maximum
Inlet concentration	10	1,000	10	1,000
pH	1	11	1	11
Adsorbent dosage	0.1	2.2	0.1	2.2
Contact time	0.25	4	0.25	4

Table 5 Optimum parameters for obtaining the maximum adsorption capacity

	Zn(II)	CBG
Inlet concentration (mg L ⁻¹)	1,000	1,000
pH	6.349	10.99
Adsorbent dosage (g L ⁻¹)	0.2363	2.20
Contact time (h)	4.5	4.5

desirable to utilize the adsorbent, best of its capability. There are several optimization techniques available such as Differential evolution, Genetic algorithm, Microsoft Solver, etc. to estimate the optimum parameters. In the present work, Microsoft Solver of Microsoft Office 2007 is utilized for evaluating the optimal parameters. The optimization is carried out using the boundary conditions stated in Table 4.

The optimum parameters obtained after the implementation of Microsoft Solver are being tabulated in Table 5.

Conclusions

Alumina nanoparticles adsorbent is synthesized using solution combustion synthesis method and successfully

utilized for the removal of Zn(II) and CBG dye. The equilibrium contact time for the adsorption of Zn(II) and CBG is obtained as approximately 4.5 h. The maximum percentage removal is found as 33.5 and 25.6 % by keeping the initial concentration as 500 and 100 mg L⁻¹ for Zn(II) and CBG, respectively. The removal of Zn(II) increases with an increase in the pH of the solvent, while the removal of CBG decreases for the same. The Langmuir isotherm model describes the phenomenon for the removal of Zn(II) and CBG using the alumina nanoparticles. This supports the formation of monolayer during the adsorption process. The maximum adsorption capacity evaluated from the Langmuir isotherm model is 1,047.83 and 263.16 mg g⁻¹ for the removal of Zn(II) and CBG, respectively. The maximum adsorption capacity obtained for the removal of Zn(II) and CBG using alumina nanoparticles are much higher in comparison to the other adsorbents used for the removal of metal and dyes in the industries. The removal of Zn(II) and CBG are governed by the pseudo-first-order kinetic model. Experimental data are regressed to develop the mathematical models for Zn(II) and CBG adsorption. The Microsoft Solver technique is utilized to obtain the optimum values of initial concentration, pH, contact time and adsorbent dosage for maximum adsorption capacity.

Open Access This article is distributed under the terms of the Creative Commons Attribution License which permits any use, distribution, and reproduction in any medium, provided the original author(s) and the source are credited.

References

- Maheshwari U (2013) A review on adsorption process for the removal of dyes from textile industry effluent. Paper presented at the 2013 AIChE Annual Meeting, San Francisco, CA, USA, Nov 3–8
- Gupta VK, Ali I, Saleh TA, Nayak A, Agarwal S (2012) Chemical treatment technologies for waste-water recycling—an overview. *RSC Adv* 2(16):6380–6388. doi:10.1039/c2ra20340e
- Nethaji S, Sivasamy A, Thennarasu G, Saravanan S (2010) Adsorption of Malachite Green dye onto activated carbon derived from Borassus aethiopicum flower biomass. *J Hazard Mater* 181(1–3):271–280. doi:10.1016/j.jhazmat.2010.05.008
- Mittal A, Mittal J, Malviya A, Gupta VK (2009) Adsorptive removal of hazardous anionic dye “Congo red” from wastewater using waste materials and recovery by desorption. *J Colloid Interf Sci* 340(1):16–26. doi:10.1016/j.jcis.2009.08.019
- Chatha SAS, Asgher M, Ali S, Hussain AI (2012) Biological color stripping: a novel technology for removal of dye from cellulose fibers. *Carbohydr Polym* 87(2):1476–1481. doi:10.1016/j.carbpol.2011.09.041
- Gupta S, Maheshwari U (2014) Copper (II) removal using activated neem bark from waste water as a low cost adsorbent: column studies. Paper presented at the 2014 AIChE Annual Meeting, Atlanta, GA, USA, Nov 16–21
- Maheshwari U, Gupta S (2011) Kinetic and equilibrium studies of Cr(VI) removal from aqueous solutions using activated neem bark. *Res J Chem Env* 15(2):939–943
- Gangwar DKK (2010) Metals concentration in textile and tannery effluents, associated soils and ground water. *NY Sci J* 3(4)
- Thippeswamy B, Shivakumar CK, Krishnappa M (2012) Accumulation potency of heavy metals by *saccharomyces* sp. Indigenous to paper mill effluent. *J Environ Res Dev* 6(3):439–445
- Gangadhar G, Maheshwari U, Gupta S (2012) Application of nanomaterials for the removal of pollutants from effluent streams. *Nanosci Nanotech Asia* 2:140–150. doi:10.2174/2210681211202020140
- Gupta S, Babu BV (2009) Removal of toxic metal Cr(VI) from aqueous solutions using sawdust as adsorbent: equilibrium, kinetics and regeneration studies. *Chem Eng J* 150(2–3):352–365. doi:10.1016/j.cej.2009.01.013
- Gupta VK, Jain R, Mittal A, Saleh TA, Nayak A, Agarwal S, Sikarwar S (2012) Photo-catalytic degradation of toxic dye amaranth on TiO₂/UV in aqueous suspensions. *Mater Sci Eng C* 32(1):12–17. doi:10.1016/j.msec.2011.08.018
- Gupta VK, Jain R, Nayak A, Agarwal S, Shrivastava M (2011) Removal of the hazardous dye—Tartrazine by photodegradation on titanium dioxide surface. *Mater Sci Eng C* 31(5):1062–1067. doi:10.1016/j.msec.2011.03.006
- Saleh TA, Gupta VK (2012) Photo-catalyzed degradation of hazardous dye methyl orange by use of a composite catalyst consisting of multi-walled carbon nanotubes and titanium dioxide. *J Colloid Interf Sci* 371(1):101–106. doi:10.1016/j.jcis.2011.12.038
- Shek T-H, Ma A, Lee VKC, McKay G (2009) Kinetics of zinc ions removal from effluents using ion exchange resin. *Chem Eng J* 146(1):63–70. doi:10.1016/j.cej.2008.05.019
- Karthikeyan S, Gupta VK, Boopathy R, Titus A, Sekaran G (2012) A new approach for the degradation of high concentration of aromatic amine by heterocatalytic Fenton oxidation: kinetic and spectroscopic studies. *J Mol Liq* 173:153–163. doi:10.1016/j.molliq.2012.06.022
- Xu P, Zeng GM, Huang DL, Lai C, Zhao MH, Wei Z, Li NJ, Huang C, Xie GX (2012) Adsorption of Pb(II) by iron oxide nanoparticles immobilized *Phanerochaete chrysosporium*: equilibrium, kinetic, thermodynamic and mechanisms analysis. *Chem Eng J* 203:423–431. doi:10.1016/j.cej.2012.07.048
- Xu P, Zeng GM, Huang DL, Feng CL, Hu S, Zhao MH, Lai C, Wei Z, Huang C, Xie GX, Liu ZF (2012) Use of iron oxide nanomaterials in wastewater treatment: a review. *Sci Total Environ* 424:1–10. doi:10.1016/j.scitotenv.2012.02.023
- Y-j Xu, Rosa A, Liu X, Su D-S (2011) Characterization and use of functionalized carbon nanotubes for the adsorption of heavy metal anions. *New Carbon Mater* 26(1):57–62. doi:10.1016/S1872-5805(11)60066-8
- Saleh T, Gupta V (2012) Column with CNT/magnesium oxide composite for lead(II) removal from water. *Environ Sci Pollut Res* 19(4):1224–1228. doi:10.1007/s11356-011-0670-6
- Gupta VK, Srivastava SK, Mohan D, Sharma S (1997) Design parameters for fixed bed reactors of activated carbon developed from fertilizer waste for the removal of some heavy metal ions. *Waste Manag* 17(8):517–522. doi:10.1016/S0956-053X(97)10062-9
- Gupta VK, Agarwal S, Saleh TA (2011) Synthesis and characterization of alumina-coated carbon nanotubes and their application for lead removal. *J Hazard Mater* 185(1):17–23. doi:10.1016/j.jhazmat.2010.08.053
- Mahmood T, Saddique MT, Naeem A, Mustafa S, Zeb N, Shah KH, Waseem M (2011) Kinetic and thermodynamic study of Cd(II), Co(II) and Zn(II) adsorption from aqueous solution by NiO. *Chem Eng J* 171(3):935–940. doi:10.1016/j.cej.2011.04.043
- Gupta VK, Nayak A (2012) Cadmium removal and recovery from aqueous solutions by novel adsorbents prepared from orange peel and Fe₂O₃ nanoparticles. *Chem Eng J* 180:81–90. doi:10.1016/j.cej.2011.11.006

25. Li Y, Yue Q, Gao B (2010) Adsorption kinetics and desorption of Cu(II) and Zn(II) from aqueous solution onto humic acid. *J Hazard Mater* 178(1–3):455–461. doi:10.1016/j.jhazmat.2010.01.103
26. Sheela T, Nayaka YA, Viswanatha R, Basavanna S, Venkatesha TG (2012) Kinetics and thermodynamics studies on the adsorption of Zn(II), Cd(II) and Hg(II) from aqueous solution using zinc oxide nanoparticles. *Powder Technol* 217:163–170. doi:10.1016/j.powtec.2011.10.023
27. Wang X, Li Y (2011) Measurement of Cu and Zn adsorption onto surficial sediment components: new evidence for less importance of clay minerals. *J Hazard Mater* 189(3):719–723. doi:10.1016/j.jhazmat.2011.03.045
28. Mishra AK, Arockiadoss T, Ramaprabhu S (2010) Study of removal of azo dye by functionalized multi walled carbon nanotubes. *Chem Eng J* 162(3):1026–1034. doi:10.1016/j.cej.2010.07.014
29. Madrakian T, Afkhami A, Ahmadi M, Bagheri H (2011) Removal of some cationic dyes from aqueous solutions using magnetic-modified multi-walled carbon nanotubes. *J Hazard Mater* 196:109–114. doi:10.1016/j.jhazmat.2011.08.078
30. Mittal A, Mittal J, Malviya A, Kaur D, Gupta VK (2010) Decoloration treatment of a hazardous triarylmethane dye, Light Green SF (Yellowish) by waste material adsorbents. *J Colloid Interf Sci* 342(2):518–527. doi:10.1016/j.jcis.2009.10.046
31. Mittal A, Kaur D, Malviya A, Mittal J, Gupta VK (2009) Adsorption studies on the removal of coloring agent phenol red from wastewater using waste materials as adsorbents. *J Colloid Interf Sci* 337(2):345–354. doi:10.1016/j.jcis.2009.05.016
32. Mittal A, Mittal J, Malviya A, Gupta VK (2010) Removal and recovery of Chrysoidine Y from aqueous solutions by waste materials. *J Colloid Interf Sci* 344(2):497–507. doi:10.1016/j.jcis.2010.01.007
33. Jain AK, Gupta VK, Bhatnagar A, Suhas (2003) A comparative study of adsorbents prepared from industrial wastes for removal of dyes. *Sep Sci Technol* 38(2):463–481. doi:10.1081/ss-120016585
34. Aruna ST, Mukasyan AS (2008) Combustion synthesis and nanomaterials. *Current Opin Solid State Mater Sci* 12(3–4): 44–50. doi:10.1016/j.cossms.2008.12.002
35. Mimani T, Patil KC (2001) Solution combustion synthesis of nanoscale oxides and their composites. *Mater Phys Mech* 4(2): 134–137
36. Cash PD (2008) EDTA Titrations 1: Standardization of EDTA and analysis of Zinc in a Supplement Tablet. <http://www.uclmail.net/users/dn.cash/EDTA1.pdf>. Accessed 28 Mar 2011
37. Gupta S, Babu BV (2009) Utilization of waste product (tamarind seeds) for the removal of Cr(VI) from aqueous solutions: Equilibrium, kinetics, and regeneration studies. *J Environ Manag* 90(10):3013–3022. doi:10.1016/j.jenvman.2009.04.006
38. Gupta S, Babu BV (2010) Experimental, kinetic, equilibrium and regeneration studies for adsorption of Cr(VI) from aqueous solutions using low cost adsorbent (activated flyash). *Desalin Water Treat* 20(1–3):168–178. doi:10.5004/dwt.2010.1546
39. Kyzas GZ, Siafaka PI, Pavlidou EG, Chrissafis KJ, Bikiaris DN (2015) Synthesis and adsorption application of succinyl-grafted chitosan for the simultaneous removal of zinc and cationic dye from binary hazardous mixtures. *Chem Eng J* 259:438–448. doi:10.1016/j.cej.2014.08.019
40. Saikia J, Sikdar Y, Saha B, Das G (2013) Malachite nanoparticle: A potent surface for the adsorption of xanthene dyes. *J Environ Chem Eng* 1(4):1166–1173. doi:10.1016/j.jece.2013.09.002
41. Gong J-L, Wang X-Y, Zeng G-M, Chen L, Deng J-H, Zhang X-R, Niu Q-Y (2012) Copper (II) removal by pectin-iron oxide magnetic nanocomposite adsorbent. *Chem Eng J* 185–186: 100–107. doi:10.1016/j.cej.2012.01.050
42. Cardoso NF, Pinto RB, Lima EC, Calvete T, Amavisca CV, Royer B, Cunha ML, Fernandes THM, Pinto IS (2011) Removal of remazol black B textile dye from aqueous solution by adsorption. *Desalination* 269(1–3):92–103. doi:10.1016/j.desal.2010.10.047
43. Babu BV, Gupta S (2008) Removal of Cr(VI) from wastewater using activated tamarind seeds as an adsorbent. *J Environ Eng Sci* 7(5):553–557
44. Bhattacharyya K, Gupta S (2006) Adsorption of Fe(III) from water by natural and acid activated clays: studies on equilibrium isotherm, kinetics and thermodynamics of interactions. *Adsorption* 12(3):185–204. doi:10.1007/s10450-006-0145-0
45. Babu BV, Gupta S (2008) Adsorption of Cr(VI) using activated neem leaves as an adsorbent: kinetic studies. *Adsorption* 3(1):85–92

